Association of calnexin with mutant peripheral myelin protein-22 *ex vivo*: A basis for "gain-of-function" ER diseases

K. M. Dickson*, J. J. M. Bergeron†‡, I. Shames§, J. Colby§, D. T. Nguyen¶, E. Chevet¶, D. Y. Thomas†‖, and G. J. Snipes*†§

Departments of *Neurology and Neurosurgery, †Anatomy and Cell Biology, §Pathology, ¶Surgery, and ‖Biochemistry, McGill University, 3640 University Street, Montreal, QC, Canada H3A 2B2

Edited by Kai Simons, Max Planck Institute of Molecular Cell Biology and Genetics, Dresden, Germany, and approved May 17, 2002 (received for review November 22, 2001)

Schwann cell-derived peripheral myelin protein-22 (PMP-22) when mutated or overexpressed causes heritable neuropathies with a previously unexplained "gain-of-function" endoplasmic reticulum (ER) retention phenotype. In wild-type sciatic nerves, PMP-22 associates in a specific, transient ($t_{1/2} \approx 11$ min), and oligosaccharide processing-dependent manner with the lectin chaperone calnexin (CNX), but not calreticulin nor BiP. In *Trembler-J* (*Tr-J*) sciatic nerves, prolonged association of mutant PMP-22 with CNX is found ($t_{1/2} > 60$ min). In 293A cells overexpressing PMP-22$^{Tr\text{-}J}$, CNX and PMP-22 colocalize in large intracellular structures identified at the electron microscopy level as myelin-like figures with CNX localization in the structures dependent on PMP-22 glucosylation. Similar intracellular myelin-like figures were also present in Schwann cells of sciatic nerves from homozygous *Trembler-J* mice with no detectable activation of the stress response pathway as deduced from BiP and CHOP expression. Sequestration of CNX in intracellular myelin-like figures may be relevant to the autosomal dominant Charcot–Marie–Tooth-related neuropathies.

endoplasmic reticulum quality control | myelinopathy | hereditary neuropathy | Trembler | Charcot–Marie–Tooth disease

Defects in the gene for the polytypic integral membrane protein peripheral myelin protein 22 (PMP-22) of the myelin sheath are responsible for the Trembler (Tr) and Trembler-J (Tr-J) neuropathies in mice and Charcot–Marie–Tooth disease, hereditary neuropathy with liability to pressure palsies, and Dejerine–Sottas syndrome in humans. The function of PMP-22 is unknown, but roles in cell growth, apoptosis, higher order macromolecular structure, and intracellular signaling have been proposed (1). Intrachromosomal duplications (2) and deletions (3) encompassing PMP-22 cause Charcot–Marie–Tooth disease and hereditary neuropathy with liability to pressure palsies, respectively. In addition, point mutations have been found in patients with Charcot–Marie–Tooth disease, hereditary neuropathy with liability to pressure palsies, and Dejerine–Sottas syndrome (4). Indeed, the first missense mutations to be identified in the PMP-22 gene were found in the Tr (5) and Tr-J (6) mice with identical point mutations shared between humans and mice (7, 8).

Many PMP-22 mutations are retained intracellularly (9–12) and appear to belong to a growing class of mutations termed "endoplasmic reticulum (ER) retention mutations" that are recognized by ER resident-folding proteins, molecular chaperones, and/or other enzymes that serve to monitor the fidelity of protein synthesis and macromolecular assembly (13, 14). Among ER retention diseases, however, heritable neuropathies caused by PMP-22 mutation or overexpression are unique because they are dominant gain-of-function diseases (15).

Here, transient and glucosylation-dependent association of PMP-22 with the ER chaperone calnexin (CNX) was observed. PMP-22 associated only with CNX. Formation of intracellular myelin-like figures (IMLFs) in transfected cells coincided with the cosequestration of CNX in a glucosylation dependent fashion. Similar intracellular myelin-like structures were present in the sciatic nerves of homozygous *Tr-J* mice. These results provide a mechanistic explanation for the human Charcot–Marie–Tooth disease secondary to the ER retention of mutant PMP-22 via the CNX cycle and provide an unexpected link between the gain-of-function phenotype of such diseases and sequestration of the resident ER lectin chaperone, CNX.

Materials and Methods

Metabolic Labeling, Immunoprecipitations, and Western Blot Analysis. Metabolic labeling and pulse–chase of mouse sciatic nerves and immunoprecipitations for PMP-22 (16) as well as nondenaturing CNX immunoprecipitations, BiP immunoprecipitation, and ATP depletion of cell lysates have been described (17, 18). For sequential PMP-22 immunoprecipitations, lysates were first CNX immunoprecipitated as described (17) followed by resolubilization in 0.5% SDS in 50 mM Tris (pH 8.0) and PMP-22 immunoprecipitated in modified radioimmunoprecipitation assay buffer (50 mM Tris, pH 8.0/150 mM NaCl/1% deoxycholate containing 0.5% Nonidet P-40). Samples were electrophoresed, transferred to nitrocellulose membranes, and exposed to film by using the Kodak Biomax Transcreen LE system (NEN). For some experiments, sciatic nerves were pretreated with 1 mM castanospermine (Sigma–Aldrich) for 1 h at 37°C before and during metabolic labeling. Samples were then homogenized in 2% 3-[(3-cholamidopropyl)dimethylammonio]-1-propanesulfonate lysis buffer containing 5 mM iodoacetamide and gels processed for fluorography by using EN^{3}HANCE reagent (NEN). Western blot analysis of membranes incubated in anti-PMP-22 (Susi-4; 1:500) Ab overnight or anti-PMP-22 antiserum preblocked with immunizing peptide was performed as described (19).

Immunofluorescence of Wild-Type (wt), *Tr*, and *Tr-J* PMP-22-Transfected Cells. QBT 293A, COS, or HeLa cells were transiently transfected with either C-terminal green fluorescent protein (GFP)-tagged PMP-22^{wt}, PMP-22^{Tr}-GFP, and PMP-22$^{Tr\text{-}J}$-GFP or N-glucosylation site deleted (N41A) PMP-22^{wt}-GFP. Mutagenesis of PMP-22 was obtained by using a Transformer site-directed mutagenesis kit per the manufacturer's instructions (COLETTE, Palo Alto, CA) and verified by sequencing. Cells were fixed with 4% paraformaldehyde in phosphate buffer for 15 min at room temperature. Coverslips were rinsed twice in PBS containing 0.01% Tween-20 and permeabilized 5 min in PBS containing 0.2% Triton X-100. Cells were blocked in 5% normal goat serum in PBS for 15 min followed by incubation in affinity-purified anti-CNX (αC4; 1:300) or protein disulfide isomerase (Affinity Bioreagents,

This paper was submitted directly (Track II) to the PNAS office.

Abbreviations: PMP-22, peripheral myelin protein-22; GFP, green fluorescent protein; IMLF, intracellular myelin-like figure; wt, wild type; Tr-J, Trembler-J; CST, castanospermine; ICS, intracellular structures; ER, endoplasmic reticulum; CNX, calnexin; EM, electron microscopy.

‡To whom correspondence should be addressed. E-mail: john.bergeron@mcgill.ca.

www.pnas.org/cgi/doi/10.1073/pnas.152621799

Golden, CO) for 1 h. Coverslips were washed and incubated with either Cy3-labeled donkey anti-rabbit IgG or Cy3-labeled donkey anti-mouse IgG (1:250; Jackson ImmunoResearch) for 1 h at room temperature. Confocal images were obtained on a Zeiss LSM 410 microscope. Immunofluorescence images were obtained on Zeiss axioscope. For quantitation of immunofluorescence intensity, images were obtained by using a Zeiss LSM 510 microscope. Cells expressing GFP-tagged protein were encircled and the number of pixels (minus background) and surface area (μm^2) established by using LSM 5 image examiner (Zeiss). Total fluorescence/cell was then calculated. Cells were classified by PMP-22/CNX colocalization within different compartments (i.e., plasma membrane vs. ER vs. IMLFs).

Genotyping. *Tr-J* mice (C57BL/6J) obtained courtesy of A. Peterson (Royal Victoria Hospital, Montreal) were genotyped as described (20).

Electron Microscopy (EM). 293A and HeLa cells transfected with either GFP alone, PMP-22^{wt}-GFP, or PMP-22$^{Tr\text{-}J}$ -GFP and *Tr-J* sciatic nerves were processed as described (21). For quantitation of intracellular structures (ICS), a total of 25 EM photomicrographs/transfection condition were taken wherever either IMLFs or aggresomes could be found. The percentage per intracellular structure/transfection condition was then calculated.

Reverse Transcription–PCR (RT-PCR) Analysis. Sciatic nerve and liver tissues from either wt, *Tr-J*/+, or *Tr-J*/*Tr-J* mice were pooled and homogenized in Trizol (Invitrogen). Total RNA was isolated and converted into cDNA by using oligo(dT)$_{20}$-primed oligonucleotides and the Thermoscript RT-PCR system (Invitrogen). One-eighth of the cDNA synthesis reaction was used for PCR analysis of BiP, CHOP, and glyceraldehyde-3-phosphate dehydrogenase mRNA expression by amplification with *Taq* DNA polymerase (Fermentas, Burlington, Canada). Each PCR was analyzed in the linear part of the amplification. Oligonucleotides (αDNA) used for PCR were as follows: 5′-gggaaagaaggttacccatgc and 5′-cgagtagatccaccaaccagag for BiP; 5′-ccctgcctttcaccttgg and 5′-ccgctcgttctcctgctc for CHOP; and 5′-ACCACCATGGAGAAGGCTGG and 5′-CTCAGTGTAGCCCAGGATGC for glyceraldehyde-3-phosphate dehydrogenase. PCR-amplified products were analyzed on agarose gel and quantified with FluorChem (Alphatech Innovation, Burlington, MA).

Results

CNX Association with Sciatic Nerve PMP-22 *ex Vivo*. wt PMP-22 is a multipass integral membrane protein (22) with a single site of N-glucosylation at residue N41 (23). To screen for relevant ER chaperones interacting with newly synthesized PMP-22, coimmunoprecipitation experiments with freshly excised rat sciatic nerves radiolabeled *ex vivo* were performed by using anti-CNX, anticalreticulin, and anti-BiP antisera. The major radiolabeled polypeptide that coimmunoprecipitated with CNX has a similar mobility to PMP-22 (Fig. 1*a*, compare lanes 1 and 2). Little significant association with any sciatic nerve proteins could be demonstrated in anti-calreticulin immunoprecipitates (Fig. 1*a*, lane 3) from sciatic nerves. As expected, BiP associated with substrates that were released by ATP hydrolysis (Fig. 1*a*, compare lanes 4 and 5), but these did not correspond to polypeptides with the electrophoretic mobility of PMP-22. Little radiolabel was immunoprecipitated with nonimmune serum (Fig. 1*a*, lane 6).

Confirmation of the identity of the 22-kDa polypeptide associated with CNX was revealed by Western blotting and sequential coimmunoprecipation. Immunoreactive PMP-22 was clearly detected in Western blots of total protein from rat sciatic nerves (Fig. 1*b*, lane 1) and in anti-CNX immunoprecipitates from sciatic nerve (Fig. 1*b*, lane 2), but not in sciatic nerve immunoprecipitates by using nonimmune serum (Fig. 1*b*, lane 3). As a specificity control,

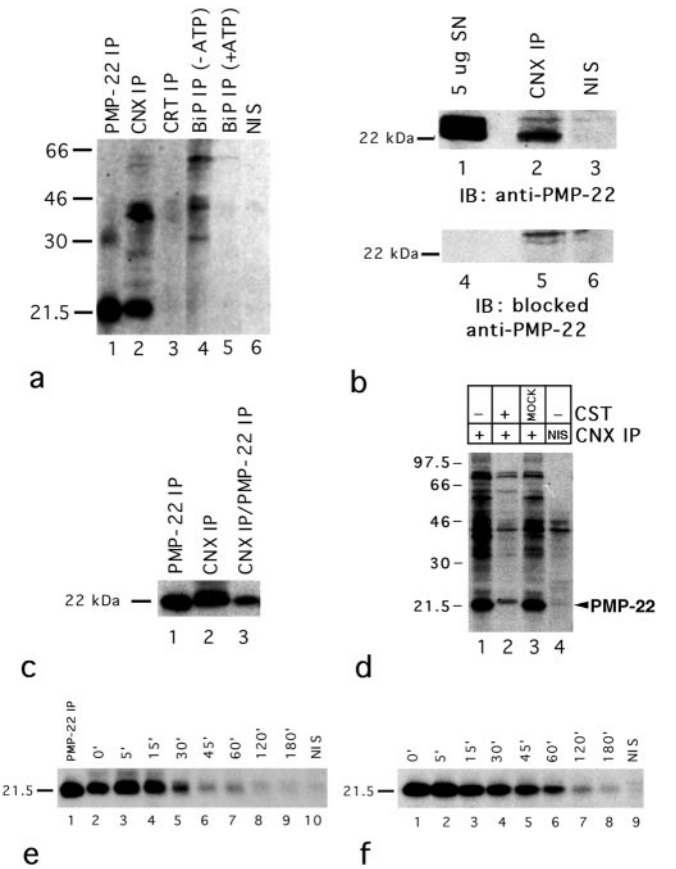

Fig. 1. CNX coimmunoprecipitation with PMP-22 in rat sciatic nerves. (*a*) Lysates (200 μg/immunoprecipitation) from metabolically labeled (0.4 mCi/ml; specific activity = 1,175 Ci/mmol) sciatic nerves were immunoprecipitated with either anti-PMP-22 (lane 1), anti-CNX (lane 2), anticalreticulin (lane 3), anti-BiP (lanes 4 and 5) Abs, or nonimmune serum (NIS; lane 6). As a specificity control, anti-BiP immunoprecipitates were incubated with Mg^{2+} ATP to release substrates because of ATPase activity (lane 5). (*b*) Unlabeled sciatic nerve lysates (400 μg/immunoprecipitation) were immunoprecipitated with either anti-CNX Ab (lanes 2 and 5) or nonimmune serum (lanes 3 and 6) and Western blotted. Total protein from rat sciatic nerves were included as positive controls (lanes 1 and 4). Blots were probed with either anti-PMP-22 (lanes 1–3) or anti-PMP-22 (lanes 4–6) preblocked with the immunizing peptide. (*c*) Metabolically labeled sciatic nerve lysates (30 min) were either immunoprecipitated with anti-PMP-22 (lane 1) or anti-CNX (lane 2). CNX immunoprecipitates were resolubilized and reimmunoprecipitated with anti-PMP-22, confirming the identity of the 22-kDa band as PMP-22 (lane 3). (*d*) Treatment of sciatic nerves with 1 mM CST 60 min before and during metabolic labeling reduced the association of PMP-22 and CNX (compare lanes 1 and 2) by 90% as determined by densitometry (data not shown). In mock CST controls (lane 3), sciatic nerves were simultaneously incubated in DMEM in the absence of CST. After treatment with/without CST, lysates were immunoprecipitated with either anti-CNX (lane 1–3) or nonimmune serum (lane 4). (*e* and *f*) Sciatic nerves were metabolically labeled and then ''chased'' with 2 mM L-methionine in DMEM for the indicated time intervals. Lysates were subsequently immunoprecipitated with anti-CNX (*e*, lanes 2–9), anti-PMP-22 (*e*, lane 1; *f*, lanes 1–8), or nonimmune serum (*e*, lane 10; *f*, lane 9). Exposure = 21 d for *a* and *d*; 10 d for *c*, *e*, and *f*.

the binding of the anti-PMP-22 Abs to PMP-22 was abrogated when immunoblots were probed with peptide-blocked anti-PMP-22 (Fig. 1*b*, lanes 4 and 5). Comparison of the 22-kDa bands found in the anti-PMP-22 immunoprecipitates (Fig. 1*c*, lane 1), the major polypeptide coimmunoprecipitated with CNX (Fig. 1*c*, lane 2), and sequential anti-PMP-22 immunoprecipitates from the CNX precipitation (Fig. 1*c*, lane 3) demonstrated that PMP-22 is a CNX substrate.

CNX specifically associates with newly synthesized monoglucosy-

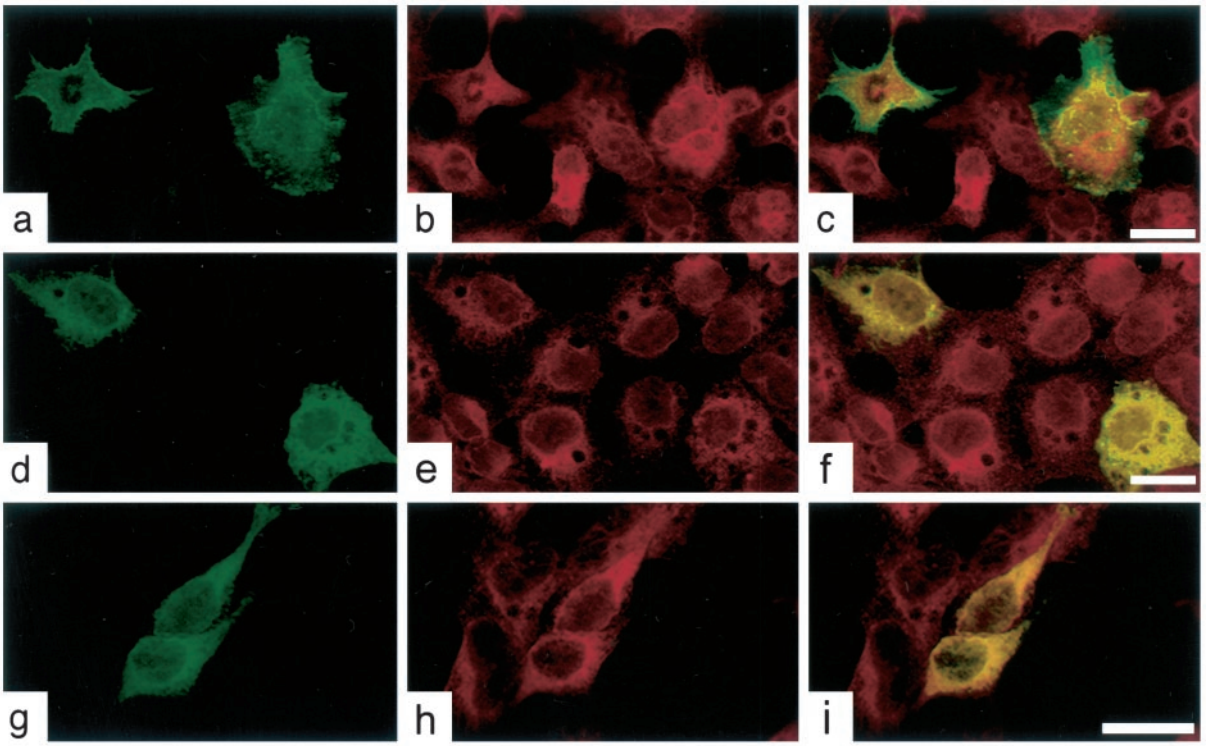

Fig. 2. CNX associates with PMP-22^{wt}, PMP-22^{Tr}, and PMP-22$^{Tr\text{-}J}$ in transiently transfected 293A cells. Cells were transfected with either PMP-22^{wt}-GFP (*a–c*), PMP-22^{Tr}-GFP (*d–f*), and PMP-22$^{Tr\text{-}J}$-GFP (*g–i*) and processed for anti-CNX immunofluorescence (*b*, *e*, and *h*). Confocal overlay images for PMP-22^{wt}-GFP and CNX show a distinct plasmalemmal colocalization (*c*). By contrast, PMP-22^{Tr}-GFP (*f*) and PMP-22$^{Tr\text{-}J}$-GFP (*i*) show a colocalization with CNX. (Bar = 25 μm.)

lated glycoproteins (13, 24, 25). Such interactions are prevented by castanospermine which inhibits glucosidase trimming of the glucosylated high mannose oligosaccharide on newly synthesized N-linked glycoproteins (26). In the presence of castanospermine (CST), PMP-22 association with CNX was reduced by 90% (Fig. 1*d*, lane 2) compared to untreated controls (Fig. 1*d*, lanes 1 and 3) as determined by densitometry (not shown). Hence, glucosidase processing of newly synthesized PMP-22 was required for CNX association.

Pulse–chase protocols were used to evaluate the kinetics of the association of PMP-22 with CNX (Fig. 1*e*). Between 5 and 45 min of chase, newly synthesized PMP-22 (30-min radiolabeling) formed a transient association with CNX (Fig. 1*e*) with a calculated $t_{1/2}$ of 11 min, whereas the half-life of newly synthesized PMP-22 in sciatic nerves is ≈30 min (Fig. 1*f*).

Visualization of Quality Control. Available Abs to PMP-22 were ineffective by immunofluorescence. Consequently, cells were transfected with either PMP-22^{wt}, PMP-22^{Tr}, or PMP-22$^{Tr\text{-}J}$ (Fig. 2) all with carboxyl termini fused to GFP. The cells were then with fixed and stained with CNX Abs by indirect immunofluorescence with Cy3. A characteristic ER reticular appearance for CNX was visualized in all cells (Fig. 2 *b*, *e*, and *h*). wt PMP-22-GFP fusion protein was localized to the plasma membrane (Fig. 2*a*), whereas plasma membrane localization was not apparent in cells expressing mutant PMP-22^{Tr}-GFP (Fig. 2*d*) and PMP-22$^{Tr\text{-}J}$-GFP (Fig. 2*g*) transfected cells. Overlay confocal images of PMP-22^{Tr}-GFP (Fig. 2*f*) and PMP-22$^{Tr\text{-}J}$-GFP (Fig. 2*i*) with CNX-Cy3 immunofluorescence showed a colocalization of the mutant PMP-22 proteins with CNX, but not that of PMP-22^{wt} (Fig. 2*c*). Parallel coimmunoprecipitation studies (not shown) revealed CNX association with wt, PMP-22^{Tr}, and PMP-22$^{Tr\text{-}J}$ in these cells.

Overexpression of wt and PMP-22$^{Tr\text{-}J}$ in different types of cells led to the formation of large ICS (arrowheads; Fig. 3*a*). Although these ICS could be quantified in 293A, COS and HeLa cells transfected with PMP-22^{wt}-GFP, the frequency of their formation increased markedly when cells were transfected with PMP-22$^{Tr\text{-}J}$-GFP (Fig. 3*b*). Both for PMP-22^{wt}-GFP and PMP-22$^{Tr\text{-}J}$-GFP transfected 293 cells, two-way ANOVA analysis of quantified intensities of GFP protein expression (total fluorescence/cell) indicated ($P < 0.001$) that cells containing ICS expressed more than cells showing a plasma membrane or only a reticular ER localization of PMP-22 (Fig. 3*c*). By immunofluorescence, these intracellular spherical bodies colocalized with CNX (Fig. 3 *d–i*). Controls with GFP alone revealed no detectable ICS whereas controls overexpressing PMP-22$^{Tr\text{-}J}$ without GFP led to a similar accumulation of ICS immunoreactive with anti-CNX (data not shown).

EM revealed that the ICS correspond to IMLFs in 293A cells overexpressing either wt (not shown) or mutant PMP-22 (Fig. 3*j*). HeLa cells transfected with PMP-22$^{Tr\text{-}J}$-GFP resulted in the formation of consistently smaller IMLFs (Fig. 3*k*), aggresomes (Fig. 3*l*), or a combination of both structures within one cell. Quantitation of ICS present in cells transfected with either GFP alone, PMP-22^{wt}-GFP or PMP-22$^{Tr\text{-}J}$-GFP revealed that 293A cells possess only IMLFs (Fig. 3*m*). A distinct pattern developed in HeLa cells transfected with either GFP alone, PMP-22^{wt}-GFP or PMP-22$^{Tr\text{-}J}$-GFP (Fig. 3*m*). Although aggresomes were commonly observed in PMP-22-transfected HeLa cells, the frequency of IMLFs is increased in HeLa cells transfected with the mutant protein. The formation of IMLFs in cells transfected with wt or mutant PMP-22-GFP and their absence in either 293 cells and HeLa cells transfected with GFP alone provides further evidence that tagging PMP-22 with GFP at the C terminus does not affect its trafficking. Remarkably, aggresomes were observed in HeLa cells transfected with GFP alone but were absent in 293 cells transfected with GFP or the PMP-22-GFP constructs (Fig. 3*m*). Hence, IMLFs, but not aggresomes, coincided with overexpression of wt or mutant PMP-22.

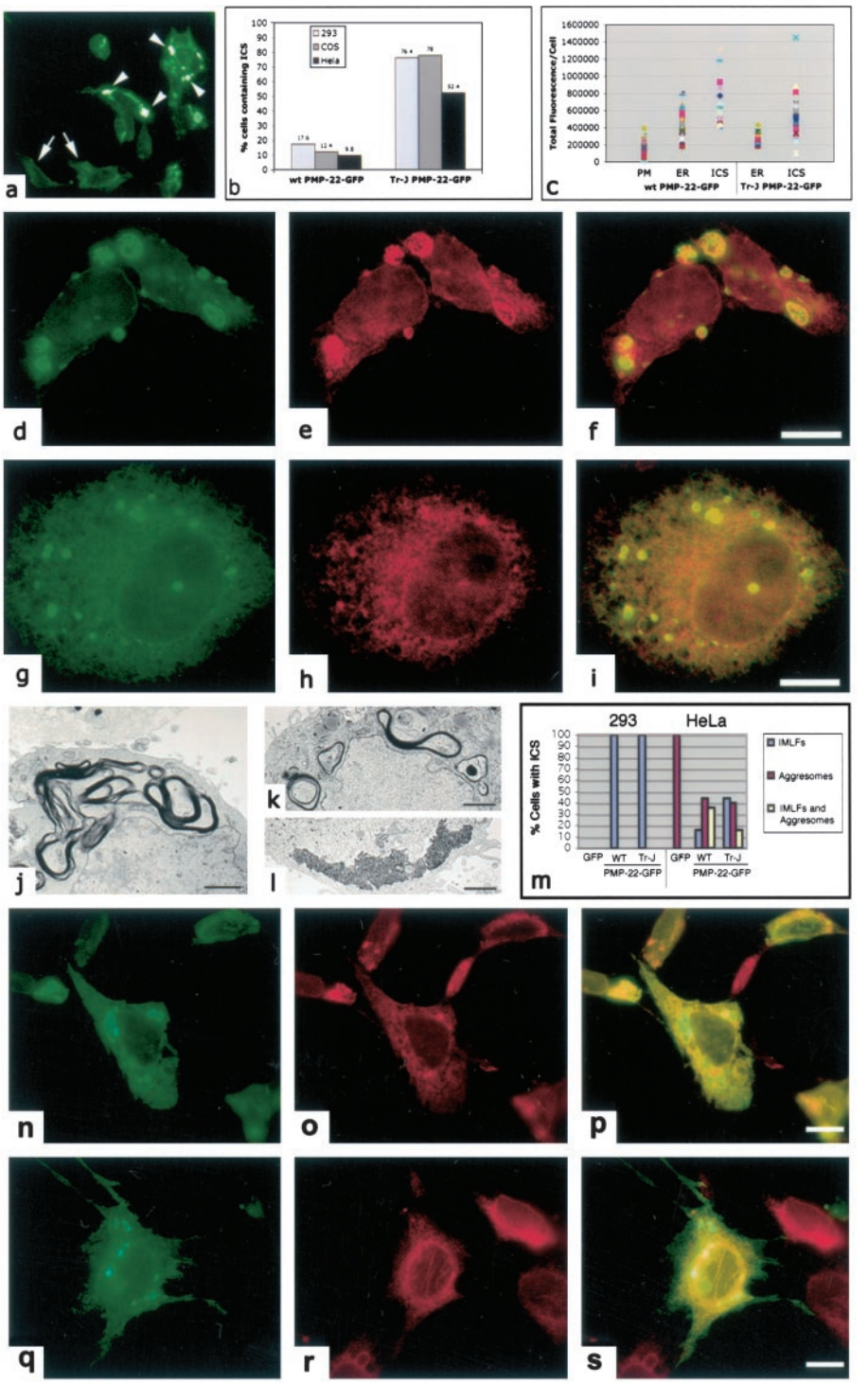

Fig. 3. CNX colocalizes with IMLFs in cells overexpressing PMP-22^{wt} and PMP-22$^{Tr\text{-}J}$. (*a*) The presence of large ICS (arrowheads) within 293 cells transiently transfected with PMP-22$^{Tr\text{-}J}$ -GFP in comparison to cells having an ER-like localization of the PMP-22-GFP protein (arrows). Quantitation (total of 1,000 cells counted/cell-type) of the presence of ICS/cell-type confirmed the greater incidence of these structures residing in cells transfected with mutant PMP-22$^{Tr\text{-}J}$-GFP as compared to cells transfected with PMP-22^{wt}-GFP (*b*). The total fluorescence/cell (*c*; described in *Materials and Methods*) assessed the level of PMP-22-GFP protein expression in transfected 293 cells with either plasma membrane (PM), ER, or ICS scored. Two-way ANOVA determined the amounts of PMP-22^{wt}-GFP protein expressed with PM, ER, and ICS localizations as significantly different ($P < 0.001$). Likewise, the amounts of PMP-22$^{Tr\text{-}J}$-GFP protein with ER and ICS localizations were also significantly different ($P < 0.001$). Immunofluorescence microscopy of transfected 293A (*d–f*) and HeLa (*g–i*) cells revealed a colocalization of CNX with ICS in cells overexpressing PMP-22$^{Tr\text{-}J}$-GFP (*f* and *i*). EM of 293A cells overexpressing PMP-22$^{Tr\text{-}J}$-GFP, revealed the ultrastructure of these IMLFs in the cytoplasm of cells (*j*). Conversely, HeLa cells transfected with PMP-22$^{Tr\text{-}J}$-GFP led to the formation of either IMLFs (*k*), aggresomes (*l*), or a combination of both structures within one cell (see *m*). Although aggresomes could be found in all transfected HeLa cells, no aggresomes were seen in 293 cells (*m*). Immunofluorescence of the ER protein disulfide isomerase (*o*) did not reveal a colocalization with IMLFs (*n* and *p*). Removal of the N-linked glucosylation site (N41A) of PMP-22^{wt}-GFP revealed ICS (*q*) but these were unreactive for CNX (*r* and *s*) revealing that formation of IMLFs was not dependent on its association. (Bar = *d–f* and *g–i*,15 μm; *j*, *k*, and *l*, 2 μm; and *n–s*, 15 μm.)

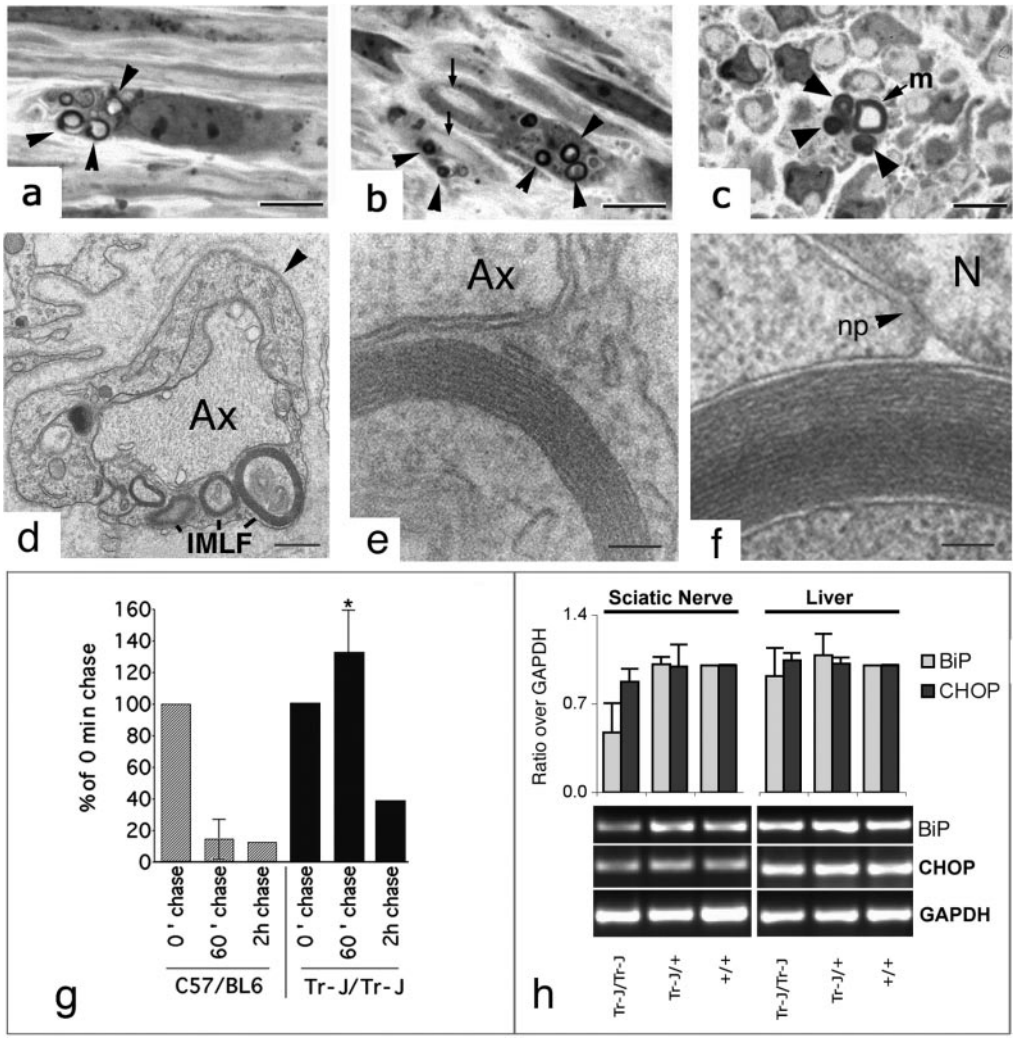

Fig. 4. Presence of IMLFs in *Tr-J/Tr-J* nerves and prolonged association of CNX with PMP-22$^{Tr\text{-}J}$ *in vivo*. IMLFs were visualized in Schwann cells of *Tr-J* homozygous mice at the light microscope (*a–c*) and EM levels (*d–f*). (*a*) IMLFs (arrowheads) present in a perinuclear position of a Schwann cell. (*b*) IMLFs (arrowheads) in Schwann cells and the consequent lack of myelination in nearby axons (arrows). (*c*) Cross section of a partially myelinated fiber (m) and a closely associated Schwann cell with IMLFs (arrowheads). (*d*) IMLFs in a Schwann cell identified by its basal lamina (arrowhead). An unmyelinated axon (Ax) is indicated. At higher magnification (*e*), parallel arrays of membranes in an IMLF of the Schwann cell can be visualized. The ultrastructure of the IMLF seen in *Tr-J* sciatic nerves (*e*) is similar to that seen in 293 cells overexpressing PMP-22$^{Tr\text{-}J}$-GFP (*f*). (*g*) Sciatic nerves from wt and *Tr-J/Tr-J* mice were pulse-labeled for 30 min with Tran^{35}S-label (0.4 mCi/ml; specific activity = 1,175 Ci/mmol) chased with 2 mM L-methionine supplemented DMEM for either 60 or 120 min, followed by immunoprecipitation of lysates with anti-CNX. In wt (C57BL/6) sciatic nerves, the association of PMP-22^{wt} and CNX is greatly diminished after a 60-min chase period, as evaluated by densitometry. In *Tr-J/Tr-J* sciatic nerves, PMP-22$^{Tr\text{-}J}$/CNX associations are not significantly decreased until 120 min after chase. The SD for the 60-min time point is shown. Data points (taken from three separate experiments; three animals/experiment) at the 60-min time point in *Tr-J/Tr-J* animals were significantly different from wt control (*, $P < 0.001$). (*h*) Relative expression levels of BiP and CHOP (normalized to glyceraldehyde-3-phosphate dehydrogenase) in wt, heterozygous, and homozygous *Tr-J* mice showed no increase in CHOP mRNA levels, indicating a lack of an unfolded protein response in *Tr-J/Tr-J* sciatic nerves (*h*). Values ± half variation are the mean of two PCRs performed for sciatic nerve and liver, respectively. m, myelinated fiber; Ax, axon; np, nuclear pore; N, nucleus. (Bar = *a–c*, 5 μm; *d*, 2 μm; and *e* and *f*, 100 nm.)

These structures, however, did not colocalize with protein disulfide isomerase, another ER resident protein, (Fig. 3 *n–p*). In addition, mutation of the N-glucosylation site of PMP-22 (N41A) expected to abolish CNX/PMP-22 associations (17) still led to the formation of abnormal PMP-22-containing ICS but without CNX accumulation (Fig. 3 *q–s*). Taken together, these studies represent the first observation of N-glucosylation-dependent sequestration of CNX by a misfolded substrate.

Presence of IMLFs in *Tr-J* Mice and Extended Association of Mutant PMP-22 with CNX *in Vivo*. The presence of myelin-like figures in *Tr-J/Tr-J* sciatic nerves was confirmed both at the light microscope (Fig. 4 *a–c*) and the EM levels (Fig. 4 *d* and *e*). At higher magnification, myelin-like figures from *Tr-J/Tr-J* homozygous sciatic nerves (Fig. 4*e*) show comparable ultrastructures to those found in 293A cells transfected with PMP-22$^{Tr\text{-}J}$-GFP with the latter demonstrating a clear ER intraluminal accumulation of myelin-like figures (Fig. 4*f*).

Misfolded proteins associate with CNX for longer times than their correctly folded counterparts as a consequence of extensive recycling through the CNX cycle (13, 17). Pulse–chase analysis (Fig. 4*g*) of CNX immunoprecipitations from wt (C57BL/6) and mutant *Tr-J/Tr-J* nerves radiolabeled *ex vivo* revealed little detectable CNX associated PMP-22^{wt} by 60 min of chase. In contrast, in *Tr-J* mice, CNX/PMP-22 association was prolonged and only decreased by 120 min after chase. Remarkably, prolonged association of PMP-22$^{Tr\text{-}J}$ with CNX did not induce an unfolded protein response as verified by quantitation of BiP and CHOP expression by reverse transcription–PCR (Fig. 4*h*).

Discussion

These results show that the lectin chaperone CNX associates transiently with PMP-22 during normal productive folding and more prolonged with mutant PMP-22 during quality control. Furthermore, the ultrastructural observations on transfected 293A cells suggest that PMP-22 directly organizes membranes into parallel arrays resembling myelin, consistent with its postulated role in myelin formation. Unexpectedly, such intracellular membrane arrays sequester CNX providing a novel explanation for gain of function diseases exemplified by the Charcot–Marie–Tooth syndrome caused by either overexpression of PMP-22 or expression of mutant protein.

The association of newly synthesized PMP-22 with CNX was transient and depended on the activity of glucosidases I and II, as predicted (13, 24), from the lectin domain of CNX interacting with a single Glc1Man9GlcNAc2 oligosaccharide at position N41 of PMP-22. This oligosaccharide is modeled at ≈12-aa residues from the phospholipid bilayer as deduced from topological studies of PMP-22 (22, 27). The recently solved x-ray crystal structure of CNX reveals its glucose-binding site to be positioned in a pocket 28 Å from the phospholipid bilayer as inferred from the position of the predicted single transmembrane domain of CNX (28). Hence the relative CNX specificity for associating with nascent PMP-22 compared to BiP and calreticulin is likely because of the inability of the oligosaccharide-containing domain of PMP-22 to reach far enough into the lumen of the ER to engage the soluble molecular chaperones (i.e., BiP and calreticulin) in the matrix of the ER (29).

IMLFs were formed when 293A cells were transfected with mutant PMP-22$^{Tr\text{-}J}$, and to a lesser extent, wt PMP-22. By fluorescence microscopy, both CNX and PMP-22$^{Tr\text{-}J}$ colocalized in structures likely to correspond to IMLFs seen in Schwann cells of *Tr-J/Tr-J* mice. However, the colocalization with CNX, but not the generation of IMLFs, depended on PMP-22 N-glycosylation.

The formation of IMLFs may be a response to mask luminal exposed stretches of hydrophobic amino acids in mutant PMP-22 accumulating in the ER because of quality control. Indeed assembly of PMP-22 into parallel membrane arrays seen as IMLFs in Schwann cells of *Tr-J* mice (Fig. 4*e*) as well as 293 cells (where the only Schwann cell protein introduced is PMP-22; Fig. 4*f*) implicates PMP-22 in membrane organization in the mechanism of myelin formation, a function previously predicted (30) but without direct evidence before these observations. Moreover, the accumulation of ER intraluminal myelin-like figures with overexpression of mutant or wt PMP-22 in 293 cells occurs despite the lack of gangliosides or other myelin proteins in the ER of 293 cells.

Myelin-like figures, similar to those observed here, have recently been described in mice overexpressing PMP-22^{wt} (31). Both *Tr* and *Tr-J* mutations are considered as gain-of-function mutations (15), which may be a consequence of sequestration of CNX by mutant PMP-22$^{Tr\text{-}J}$. However CNX was not required for the formation of ICS in 293 cells because the nonglucosylated N41A mutant of PMP-22 formed the ICS without CNX recruitment. Furthermore, other ER resident proteins such as protein disulfide isomerase were not recruited to ICS.

The endosomal/lysosomal pathway is up-regulated in the *Tr-J/+* and *Tr-J/Tr-J* mice relative to wt (20) and the IMLFs are immunoreactive to LAMP (lysosome-associated membrane protein). Hence transformation of the IMLFs into lysosomes via a well-recognized autophagic transformation (32) is the likely quality-control mechanism for the removal of mutant or overexpressed PMP-22^{wt} in at least some Charcot–Marie–Tooth syndromes. Cosequestration of CNX may deplete Schwann cells of sufficient CNX for proper quality control leading to a gain of function disease.

Aggresome formation (33) has also been postulated as a possible mechanism underlying the pathogenesis of PMP-22-related neuropathies (34). The absence of aggresomes in 293 cells and their presence in transfected HeLa cells provides evidence that disposal mechanisms are cell type specific. To date, EM studies have failed to demonstrate the presence of aggresomes in myelinating *Tr-J/Tr-J* Schwann cells or in 293 cells expressing PMP-22 and IMLFs. Finally, neither BiP nor CHOP expression increased in nerves expressing mutant PMP-22. This is not unexpected because the increased expression of these genes consequent to protein misfolding in the ER requires binding of the mutant protein to BiP (35–37) and PMP-22 appears to be a substrate only for the CNX cycle. The ER to lysosomal route for disposal of misfolded proteins predicted here may be a more general feature of quality control, namely to deal with intraluminal misfolded protein aggregates inhibited from entering the proteasomal pathway.

We thank Pamela Cameron and Ali Fazel for invaluable technical assistance, Dr. Linda Hendershot (St. Jude's Children's Hospital, Memphis, TN) for her generous contribution of anti-BiP Ab, and Drs. W. Orfali and M.-C. Guiot for genotyping of *Tr-J* animals. We also thank Dr. John Presley for his assistance in quantitative confocal microscopy. We acknowledge the assistance of the McGill University EM Center under the direction of Dr. H. Vali. The Muscular Dystrophy Association (G.J.S.) and the Canadian Institutes of Health Research (J.J.M.B. and G.J.S.) funded this work.

1. Naef, R. & Suter, U. (1998) *Microsc. Res. Tech.* **41,** 359–371.
2. Lupski, J. R., de Oca-Luna, R. M., Slaugenhaupt, S., Pentao, L., Guzzetta, V., Trask, B. J., Saucedo-Cardenas, O., Barker, D. F., Killian, J. M., Garcia, C. A., *et al.* (1991) *Cell* **66,** 219–232.
3. Chance, P. F., Alderson, M. K., Leppig, K. A., Lensch, M. W., Matsunami, N., Smith, B., Swanson, P. D., Odelberg, S. J., Disteche, C. M. & Bird, T. D. (1993) *Cell* **72,** 143–151.
4. Warner, L. E., Garcia, C. A. & Lupski, J. R. (1999) *Annu. Rev. Med.* **50,** 263–275.
5. Suter, U., Welcher, A. A., Ozcelik, T., Snipes, G. J., Kosaras, B., Francke, U., Billings-Gagliardi, S., Sidman, R. L. & Shooter, E. M. (1992) *Nature (London)* **356,** 241–244.
6. Suter, U., Moskow, J. J., Welcher, A. A., Snipes, G. J., Kosaras, B., Sidman, R. L., Buchberg, A. M. & Shooter, E. M. (1992) *Proc. Natl. Acad. Sci. USA* **89,** 4382–4386.
7. Ionasescu, V. V., Searby, C. C., Ionasescu, R., Chatkupt, S., Patel, N. & Koenigsberger, R. (1997) *Muscle Nerve* **20,** 97–99.
8. Valentijn, L. J., Baas, F., Wolterman, R. A., Hoogendijk, J. E., van den Bosch, N. H., Zorn, I., Gabreels-Festen, A. W., de Visser, M. & Bolhuis, P. A. (1992) *Nat. Genet.* **2,** 288–291.
9. D'Urso, D., Prior, R., Greiner-Petter, R., Gabreels-Festen, A. A. & Muller, H. W. (1998) *J. Neurosci.* **18,** 731–740.
10. Naef, R. & Suter, U. (1999) *Neurobiol. Dis.* **6,** 1–14.
11. Naef, R., Adlkofer, K., Lescher, B. & Suter, U. (1997) *Mol. Cell. Neurosci.* **9,** 13–25.
12. Colby, J., Nicholson, R., Dickson, K. M., Orfali, W., Naef, R., Suter, U. & Snipes, G. J. (2000) *Neurobiol. Dis.* **7,** 561–573.
13. Zapun, A., Jakob, C. A., Thomas, D. Y. & Bergeron, J. J. M. (1999) *Structure (London)* **7,** R173–R182.
14. Aridor, M. & Balch, W. E. (1999) *Nat. Med.* **5,** 745–751.
15. Snipes, G. J., Orfali, W., Fraser, A., Dickson, K. & Colby, J. (1999) *Ann. N.Y. Acad. Sci.* **883,** 143–151.
16. Pareek, S., Suter, U., Snipes, G. J., Welcher, A. A., Shooter, E. M. & Murphy, R. A. (1993) *J. Biol. Chem.* **268,** 10372–10379.
17. Ou, W. J., Cameron, P. H., Thomas, D. Y. & Bergeron, J. J. M. (1993) *Nature (London)* **364,** 771–776.
18. Oda, K., Wada, I., Takami, N., Fujiwara, T., Misumi, Y. & Ikehara, Y. (1996) *Biochem. J.* **316,** 623–630.
19. Snipes, G. J., Suter, U., Welcher, A. A. & Shooter, E. M. (1992) *J. Cell Biol.* **117,** 225–238.
20. Notterpek, L., Shooter, E. M. & Snipes, G. J. (1997) *J. Neurosci.* **17,** 4190–4200.
21. Dickson, K., Philip, A., Warshawsky, H., O'Connor-McCourt, M. & Bergeron, J. J. M. (1995) *J. Clin. Invest.* **95,** 2539–2554.
22. Taylor, V., Zgraggen, C., Naef, R. & Suter, U. (2000) *J. Neurosci. Res.* **62,** 15–27.
23. Welcher, A. A., Suter, U., De Leon, M., Snipes, G. J. & Shooter, E. M. (1991) *Proc. Natl. Acad. Sci. USA* **88,** 7195–7199.
24. Zapun, A., Petrescu, S. M., Rudd, P. M., Dwek, R. A., Thomas, D. Y. & Bergeron, J. J. M. (1997) *Cell* **88,** 29–38.
25. Parodi, A. J. (2000) *Biochem. J.* **348,** 1–13.
26. Hammond, C., Braakman, I. & Helenius, A. (1994) *Proc. Natl. Acad. Sci. USA* **91,** 913–917.
27. Suter, U. & Snipes, G. J. (1995) *J. Neurosci. Res.* **40,** 145–151.
28. Schrag, J. D., Bergeron, J. J. M., Li, Y., Borisova, S., Hahn, M., Thomas, D. Y. & Cygler, M. (2001) *Mol. Cell* **8,** 633–644.
29. Sambrook, J. F. (1990) *Cell* **61,** 197–199.
30. Snipes, G. J. & Orfali, W. (1998) *Cell Biol. Int.* **22,** 815–835.
31. Niemann, S., Sereda, M. W., Suter, U., Griffiths, I. R. & Nave, K. A. (2000) *J. Neurosci.* **20,** 4120–4128.
32. Dunn, W. A., Jr. (1990) *J. Cell Biol.* **110,** 1923–1933.
33. Johnston, J. A., Ward, C. L. & Kopito, R. R. (1998) *J. Cell Biol.* **143,** 1883–1898.
34. Notterpek, L., Ryan, M. C., Tobler, A. R. & Shooter, E. M. (1999) *Neurobiol. Dis.* **6,** 450–460.
35. Urano, F., Bertolotti, A. & Ron, D. (2000) *J. Cell Sci.* **113,** 3697–3702.
36. Ma, Y. & Hendershot, L. M. (2001) *Cell* **107,** 827–830.
37. Spear, E. & Ng, D. T. (2001) *Traffic* **2,** 515–523.